Applied and Environmental Microbiology

Influence of Substrate Mineralogy on Bacterial Mineralization of Calcium Carbonate: Implications for Stone Conservation

Carlos Rodriguez-Navarro, Fadwa Jroundi, Mara Schiro, Encarnación Ruiz-Agudo and María Teresa González-Muñoz

Appl. Environ. Microbiol. **2012, 78(11):4017. DOI: 10.1128/AEM.07044-11.**
Published Ahead of Print 23 March 2012.

AEM
Journals.ASM.org

Influence of Substrate Mineralogy on Bacterial Mineralization of Calcium Carbonate: Implications for Stone Conservation

Carlos Rodriguez-Navarro,[a] Fadwa Jroundi,[b] Mara Schiro,[a] Encarnación Ruiz-Agudo,[c]* and María Teresa González-Muñoz[b]

Departamento de Mineralogía y Petrología, Universidad de Granada, Granada, Spain[a]; Departamento de Microbiología, Universidad de Granada, Granada, Spain[b]; and Institut für Mineralogie; Universität Münster, Münster, Germany[c]

The influence of mineral substrate composition and structure on bacterial calcium carbonate productivity and polymorph selection was studied. Bacterial calcium carbonate precipitation occurred on calcitic (Iceland spar single crystals, marble, and porous limestone) and silicate (glass coverslips, porous sintered glass, and quartz sandstone) substrates following culturing in liquid medium (M-3P) inoculated with different types of bacteria (*Myxococcus xanthus*, *Brevundimonas diminuta*, and a carbonatogenic bacterial community isolated from porous calcarenite stone in a historical building) and direct application of sterile M-3P medium to limestone and sandstone with their own bacterial communities. Field emission scanning electron microscopy (FESEM), atomic force microscopy (AFM), powder X-ray diffraction (XRD), and 2-dimensional XRD (2D-XRD) analyses revealed that abundant highly oriented calcite crystals formed homoepitaxially on the calcitic substrates, irrespective of the bacterial type. Conversely, scattered spheroidal vaterite entombing bacterial cells formed on the silicate substrates. These results show that carbonate phase selection is not strain specific and that under equal culture conditions, the substrate type is the overruling factor for calcium carbonate polymorph selection. Furthermore, carbonate productivity is strongly dependent on the mineralogy of the substrate. Calcitic substrates offer a higher affinity for bacterial attachment than silicate substrates, thereby fostering bacterial growth and metabolic activity, resulting in higher production of calcium carbonate cement. Bacterial calcite grows coherently over the calcitic substrate and is therefore more chemically and mechanically stable than metastable vaterite, which formed incoherently on the silicate substrates. The implications of these results for technological applications of bacterial carbonatogenesis, including building stone conservation, are discussed.

Biomineralization of calcium carbonates, that is, the biologically controlled or mediated/induced mineralization of $CaCO_3$, is an important and ubiquitous process resulting in the production of biominerals by a range of taxa, from bacteria and archaea to eukarya (32, 53, 56, 57). Biologically controlled mineralization (BCM) of calcium carbonate involves remarkable control of size, morphology, and phase selection, resulting in complex, hierarchical organic-inorganic structures with unusual physicochemical properties (56). BCM of calcium carbonate typically takes place in eukaryotes. Examples of calcium carbonate structures formed via BCM are the shells of molluscs, sea urchin spines, and fish otoliths (53). In contrast, biologically induced mineralization (BIM) of calcium carbonate does not involve direct control of the biomineralization process by the organisms. BIM occurs either passively, due to metabolically driven changes in the chemistry of the bulk solution or around the living organisms, or actively, when the organism and/or its metabolic byproducts provide nucleation sites for mineralization (49, 58). BIM of calcium carbonate typically occurs in the presence of unicellular organisms such as bacteria (22, 31).

Calcium carbonate precipitation by a large number of bacterial genera has been observed in a range of natural environments, including soils, caves, lakes, and seawater (91), as well as in the laboratory (7, 31). Bacterial mineralization of calcium carbonates has found applications in the remediation (fixation) of metal-contaminated soil and groundwater (87), atmospheric CO_2 sequestration (21, 59), the strengthening and consolidation of soil and sand (14), the reduction of the porosity and/or permeability of geological formations (24, 29), the protection and repair of concrete and cement structures (15, 66), and the conservation of building stone and statuary (16, 19, 30, 38, 39, 40, 47, 69, 84, 88, 94). Recently, bacterial precipitation of fluorescent calcium carbonate, with potential applications as a filler in rubber, plastics, and stationery ink and as a fluorescent marker, has been reported (93).

Bacterial biomineralization of calcium carbonate, termed carbonatogenesis (47) or biocalcification (19, 94), results in the production of different phases. Calcium carbonate forms three anhydrous polymorphs (calcite, aragonite, and vaterite), two hydrated crystalline phases (monohydrocalcite [$CaCO_3 \cdot H_2O$] and ikaite [$CaCO_3 \cdot 6H_2O$]), and various amorphous phases (ACC) with differences in short-range order and degree of hydration (28, 32, 51, 67). Vaterite and calcite are the most common bacterial calcium carbonate polymorphs (4, 31, 70), although bacterial mineralization of monohydrocalcite (46) and aragonite (45, 73) has been reported. There is growing evidence that bacterial mineralization of calcium carbonate involves the formation of ACC precursor phases (4, 5, 11, 33, 60). A plausible link of calcium carbonate production to *Bacillus subtilis* genes, which may suggest that bacterial precipitation of these minerals brings some evolutionary advantage to the microorganisms, has been reported (3). For instance, calcium carbonate precipitation may help fixate excess/

Received 30 September 2011 Accepted 12 March 2012
Published ahead of print 23 March 2012
Address correspondence to Carlos Rodriguez-Navarro, carlosrn@ugr.es.
* Present address: Department of Mineralogy and Petrology, University of Granada, Granada, Spain.

doi:10.1128/AEM.07044-11

toxic Ca (60) or may help bacteria to survive unfavorable conditions in a cryptobiotic state (93). Nonetheless, viability of calcified bacterial cells for extended periods (more than 1 year) has yet to be demonstrated (94). All in all, these studies may help to explain why bacterial calcium carbonate precipitation appears to be a general, ubiquitous phenomenon (7).

Despite extensive studies on bacterial carbonatogenesis, little is known about the cause(s) of polymorph selection during bacterial calcium carbonate mineralization. One line of thought suggests that the phase and morphology of calcium carbonate are bacterium (or strain) specific (see, e.g., reference 33). In this respect, it has been reported that specific amino acid sequences in *Bacillus pasteurii* urease may be responsible for vaterite precipitation as opposed to calcite formation in the presence of other urease types (78). It has also been suggested that specific proteins in extracellular polymeric substances (EPS) produced by different types of bacteria control aragonite or calcite polymorph selection (41). Braissant et al. (9) have associated polymorph selection (vaterite versus calcite) during bacterial carbonatogenesis with the characteristics of EPS. Lian et al. (49) reported that *Bacillus megaterium* cells and EPS induce calcite and vaterite precipitation, respectively. However, Ercole et al. (23) showed that EPS isolated from *Bacillus firmus* and *Bacillus sphaericus* induce the precipitation of calcite. Tourney and Ngwenya (85) indicated that dissolved organic carbon (DOC) released from EPS produced by *Bacillus licheniformis* complexes Ca ions, reducing the calcium carbonate saturation and favoring the precipitation of calcite over that of vaterite. Chen et al. (11) suggested that differences in the composition of proteins secreted by *B. subtilis*, *Aerobacter aerogenes*, and *Proteus mirabilis* could explain differences in morphology and polymorphs (calcite versus vaterite) in carbonates produced by these bacteria. These observations may imply that carbonatogenic bacteria can exert a higher degree of control on biomineralization than previously thought, since morphology and polymorph selection are characteristics of BCM in higher-order organisms (56). However, growing evidence suggests that bacteria do not directly (or genetically) influence calcium carbonate morphology (4, 8) or polymorph selection (58, 70). In fact, it has been reported that some bacteria, such as *Myxococcus* spp., are able to induce the precipitation of either vaterite or calcite with a range of morphologies, as well as that of other minerals, such as phosphates and sulfates, depending on the composition of the culture medium (31). Nonetheless, little is known about the kinetic or thermodynamic control determining which polymorph develops upon bacterial carbonatogenesis (94). Besides its scientific interest, calcium carbonate polymorph selection can have important technical implications (57). For instance, the bacterial conservation of building stones requires the formation of a coherent, durable calcium carbonate cement. This is not fully achieved if metastable vaterite (more soluble than calcite) is formed during a bacterial conservation treatment (69). The same principle may apply to soil strengthening, cement and concrete protection, solid-phase capture of groundwater metal contaminants, and/or effective (long-term) CO_2 sequestration via bacterial calcium carbonate mineralization.

One important question that deserves further study is the role played by the solid substrate in polymorph selection during calcium carbonate precipitation induced by bacteria. This is critical, because bacteria tend to attach to solid mineral substrates (36, 37, 54), typically forming biofilms where ultimately carbonatogenesis can take place (13). It is also known that bacteria have different attachment affinities to different mineral substrates (26, 75), and such attachment typically fosters their metabolic activity and/or increases their survival rate (36, 44, 52). The study of the influence of substrate mineralogy on bacterial $CaCO_3$ mineralization may help disclose whether or not bacteria can in fact actively affect polymorph selection and may shed light on the role that substrate chemistry and structure play in bacterial calcium carbonate productivity.

Here the influence of two common mineral substrate types, calcitic and silicate substrates, on bacterial calcium carbonate precipitation and polymorph selection was studied. We strive to show that the chemical and crystallographic nature of the substrate is a key factor in polymorph selection following bacterially induced calcium carbonate precipitation. We aim at demonstrating that there is no apparent bacterial specificity in calcium carbonate polymorph selection. We also aim to show that the mineralogy of the substrate strongly affects bacterial carbonate productivity. The implications of these findings for the understanding of bacterial carbonate production in nature as well as for the technological applications of bacterial carbonatogenesis, in particular its use for stone conservation, are discussed.

MATERIALS AND METHODS

Substrates. Three types of calcitic and silicate substrates were used to fully cover the possible range of crystal sizes and pore effects that one can expect from a laboratory-based bacterial carbonatogenic experiment or from a field application of the treatment, for instance, for stone conservation. The following calcitic substrates were used. (i) In order to evaluate the possible template effect (self-epitaxy, or homoepitaxy) of the substrate on bacterial calcium carbonate mineralization, optical-quality Iceland spar single crystals (Chihuahua, Mexico) were used. The crystals were cleaved along the $\{10\ \bar{1}\ 4\}$ planes, and millimeter-sized fragments (ca. 2 by 3 by 5 mm) were obtained. (ii) To evaluate the effect of an aggregate of calcite crystals in a carbonate stone, representing a more-realistic scenario during a stone conservation treatment, Macael (Almeria, Spain) marble blocks, 1 by 1 by 0.5 cm, were prepared. Macael is a white calcitic marble profusely used in monuments and statuary in Southern Spain (e.g., the Alhambra's Court of the Lions). It displays a granoblastic texture made up of interlocking calcite crystals (0.1 to 3 mm). It is very compact and displays reduced intergranular porosity (up to 1% total porosity). Following outdoors exposure, it typically displays granular disintegration associated with a significant increase in porosity (up to 5% total porosity), an effect that often demands a conservation intervention. (iii) To evaluate the actual application of a bacterial conservation treatment on a weathered porous carbonate stone, which contains its own microbiota, calcarenite stones (limestone) from a 17th-century building (pinnacles from the Chancilleria, Granada, recently replaced during a conservation intervention) were used. Calcarenite stone blocks ca. 3 by 15 by 10 cm were prepared. Calcarenite has an average porosity of ca. 28% and a limited degree of cementation (micritic and sparitic cement) that makes this stone highly susceptible to weathering. Details on the mineralogy and texture of this stone type have been reported elsewhere (69).

To evaluate the effect of a silicate substrate on polymorph selection and texture development upon bacterial carbonate mineralization, three different silicate substrates were used: (i) silica glass coverslips (ca. 0.5 by 3 by 5 mm), (ii) 0.5-cm-tall disks of porous sintered glass (P16; Pyrex) with a diameter of 1 cm, ~28% porosity, and a mean pore radius of 3.5 μm (according to mercury intrusion porosimetry analysis), and (iii) slabs of sandstone (from Prague, Czech Republic) presenting a porosity and pore size distribution similar to those of the calcarenite stone and typically showing extensive damage (e.g., Prague's Charles Bridge) (65). Stone samples were approximately 15 by 3 by 1.5 cm. The depth of penetration

of the bacterial calcium carbonate treatment was also studied. Calcium carbonate biominerals could be easily identified on the porous silicate substrate. Note, however, that recognition of bacterial carbonates is not easy (4) and is further complicated in the case of carbonate substrates, since the substrate and the newly formed cement share the same composition and, in many cases, the same mineralogy and texture (94).

Bacterial mineralization on calcite single crystals and glass coverslips. Calcite single crystals and glass coverslips were sterilized (tyndallization) by flowing steam for 1 h at 100°C, four times in succession at 24-h intervals. Biomineralization tests were conducted in liquid medium. One single crystal or glass coverslip per test tube was used. Five milliliters of sterile M-3P culture medium [1% (wt/vol) Bacto Casitone, 1% (wt/vol) $Ca(CH_3\text{-}COO)_2 \cdot 4H_2O$ (total calcium, 43.44 mM), 0.2% (wt/vol) $K_2CO_3 \cdot 1/2H_2O$ (total potassium, 35.6 mM; total carbonate, 17.8 mM), 10 mM phosphate buffer in distilled water (pH 8)] (69) was added to each test tube. Three types of bacterial cultures were inoculated in the M-3P medium mentioned above (0.1 ml of bacterial inoculum collected at the end of the exponential-growth phase): (i) a 48-h-old *M. xanthus* culture, (ii) a 24-h-old *Brevundimonas diminuta* culture, and (iii) a 24-h-old culture of a bacterial community from weathered calcarenite stone. All inocula were prepared in M-3P medium. Uninoculated M-3P medium test tubes with either calcite single crystals or glass coverslips were used as controls for each run. A minimum of three replicates per run were performed. Crystals and coverslips were collected following 24-h (or, in the case of *M. xanthus*, 48-h) and 7-day incubation at 28°C under shaking (160 rpm) using a rotary Certomat R shaker (Braun). Collected crystals and coverslips were rinsed in distilled water, dried at room temperature, and kept in Eppendorf tubes for further analyses.

M. xanthus corresponds to strain 422 provided by the Spanish Type Culture Collection, Burjassot, Valencia, Spain. All other bacteria used were isolated from weathered calcarenite stones from the Monasterio de San Jerónimo (Granada, Spain). *B. diminuta* (strain SJ 63) was found to be the most effective of all carbonatogenic bacteria (more than 100 species) isolated from this historic building at producing calcium carbonate in M-3P medium. Details on bacterial isolation, identification, and carbonatogenic capacity have been presented elsewhere (40).

Bacterial biomineralization on marble and porous glass. Macael marble and porous glass pieces were sterilized as described above prior to biomineralization tests, which were conducted in M-3P liquid medium under static conditions (no shaking) at 28°C. One small marble or sintered glass slab per test tube with 5 ml M-3P culture medium was used in experiments. A minimum of three replicates per run were performed. The carbonatogenic microorganism used for inoculation was *M. xanthus* (a 0.1-ml inoculum). Tubes were sealed with Parafilm-covered cotton plugs after 1 week of incubation in order to avoid excessive evaporation during the extended incubation period of 28 days. Oxygen availability was ensured by the large air reservoir in the tubes. Control experiments identical to those described above were carried out without bacterial inoculation. Marble and sintered glass slabs were collected at the end of the experiment, washed thoroughly with distilled water, dried at room temperature, and stored in airtight plastic vials for further analysis.

Bacterial consolidation of limestone and sandstone blocks. Slabs of calcarenite and sandstone were treated with a sterile M-3P nutritional solution. Treatments were applied by spraying the M-3P solution onto one of the large surfaces of both types of stone. This application method mimics standard procedures used during *in situ* conservation of stone. The application of the solution was repeated twice every day for 6 days to maintain a constant dampness. A total of 1.25 ± 0.25 ml/cm^2 of M-3P solution was applied to each slab. The stones were covered throughout the treatment time to avoid the rapid evaporation of the nutritional solution and subsequent desiccation of the stones.

Mineralogical and textural analyses. Microtextural features of samples subjected to bacterial biomineralization tests were observed by scanning electron microscopy (SEM) using either a Jeol JSM5 800LV SEM, a Zeiss DSM 950 SEM, or a LEO field emission SEM (FESEM), all of them coupled with energy-dispersive spectrometry (EDS) microanalysis. Samples were coated with either gold or carbon prior to observation.

The early stages of bacterial calcium carbonate growth on the atomically flat {10 $\bar{1}$ 4} cleavage faces of calcite single crystals were studied at the nanoscale using an atomic force microscope (AFM). Crystals collected after 24 h (or 48 h) of culturing were observed on a Digital Instruments Nanoscope III Multimode AFM by working in contact mode under ambient conditions (20°C). The non-atomically-flat surfaces of the glass coverslips precluded AFM observation of the precipitates formed on such a substrate.

The mineralogy of the substrates and newly formed carbonates was determined by X-ray diffraction (XRD). The diffractometer used was a Philips PW-1710 instrument with an automatic slit, Cu Kα radiation (λ, 1.5405 Å), an explored area of 3 to 60° 2θ, and a goniometer speed of 0.05° 2θ s^{-1}. XRD goniometer calibration was performed using a silicon standard. Samples were placed in zero-background silicon sample holders without any grinding prior to analysis.

Pole figures describing the 3-dimensional (3D) orientation relationships between calcite single crystal or coverslip glass supports and the bacterial calcium carbonates formed after 1 week of culturing were determined using an X-ray single-crystal diffractometer equipped with an area detector (D8 Smart Apex; Bruker). For these 2D-XRD experiments, the working conditions were as follows: Mo Kα radiation (λ, 0.7093 Å), 50 kV and 30 mA, a pinhole collimator with a diameter of 0.5 mm, and an exposure time of 20 s per frame. Calcite single crystals and glass coverslips were measured by reflection (diffractometer ω and 2θ angles were set at 10° and 20°, respectively) while resting flat on one of the cleavage rhombohedral faces or the larger face of the coverslip, respectively. A set of frames (2D diffraction patterns) was registered while the sample was rotated around the φ angle (1 frame every 5°, for a total of 36 frames). Pole densities for the strongest reflections of calcite and vaterite were calculated and were displayed in stereographic projection using XRD2DScan software (68). Each pole figure displays the intensity variation of a given *hkl* reflection as a function of the sample orientation. From these plots, the 3D orientations of associated {*hkl*} faces were observed.

RESULTS

Bacterial mineralization on {10 $\bar{1}$ 4} faces of calcite single crystals and glass coverslips. FESEM observations showed the development of dissolution features in the control sample, where no calcium carbonate precipitate was observed after 7 days (Fig. 1a). Samples subjected to biomineralization for 7 days in the presence of *B. diminuta* (Fig. 1b) or the bacterial community (Fig. 1c) showed the formation of compact, micrometer-thick, porous $CaCO_3$ layers. About 100% surface coverage of the calcite crystal substrate by bacterial carbonates was observed with *B. diminuta*, while 85 to 95% coverage was observed in crystals cultured with the bacterial community. Such newly formed calcium carbonate layers displayed a highly preferred crystallographic orientation (Fig. 1c, arrows). Samples subjected to mineralization in the presence of *M. xanthus* showed the formation of a dense covering (70 to 100% coverage) made up of calcified bacterial cells linked by EPS (Fig. 1d). In this case it was possible to measure the surface cell density, yielding a value of $(2 \pm 0.5) \times 10^9$ cells/cm^2. 2D-XRD analyses showed the formation of oriented bacterial calcite on the calcite single crystals irrespective of the bacterial type. This was demonstrated by the absence of Debye rings in the diffraction pattern obtained following the addition of all collected patterns for φ ranging from 0 to 180° (Fig. 2a). Pole figures showed that bacterial calcite displayed a preferred crystallographic orientation with the [104] pole parallel to the [104] pole of the calcite substrate (Fig. 2b).

AFM analyses revealed that at the early stages of biomineral-

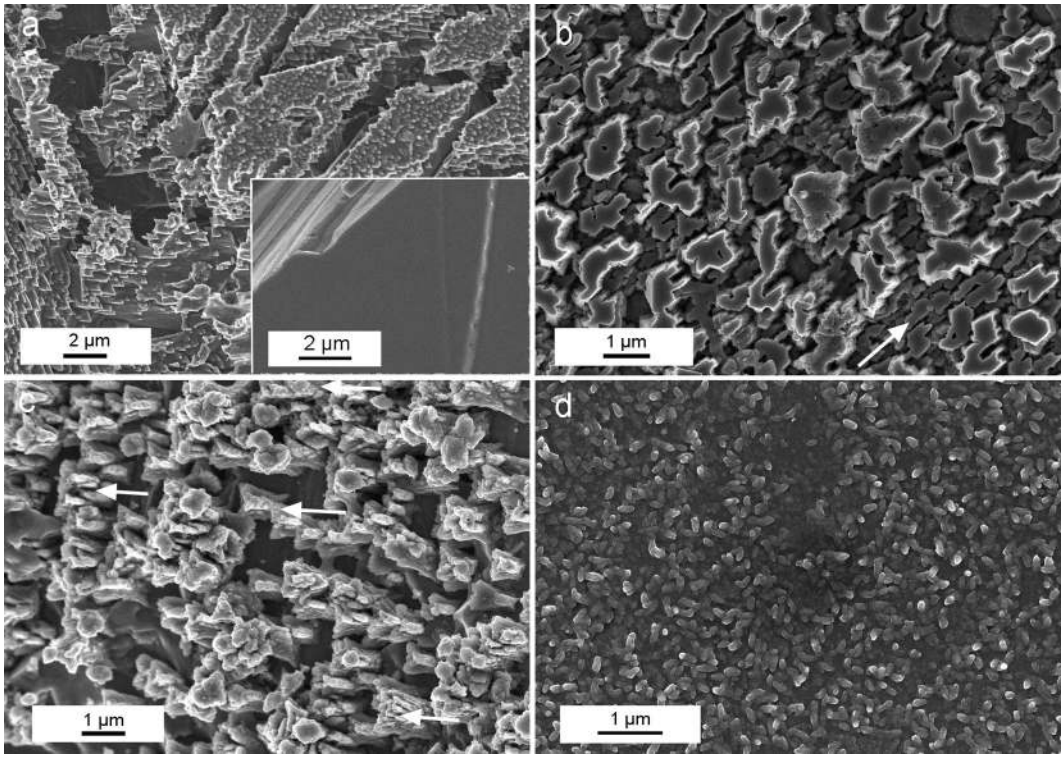

FIG 1 FESEM images of {10 $\bar{1}$ 4} faces of calcite single crystals subjected to bacterial mineralization. (a) Control showing extensive dissolution features, including cracks parallel to the rhombohedral cleavage planes. (Inset) Surface of the calcite crystal prior to experiments. (b) Calcium carbonate overgrowth formed in the presence of *B. diminuta*. Note the preferred orientation of the precipitates (arrow). (c) Well-aligned calcium carbonate precipitates (arrows indicate some examples of oriented overgrowth) formed in the presence of the bacterial consortium. (d) Massive layer of calcified *M. xanthus* cells.

ization (24 h or 48 h), the newly formed precipitates grew in good crystallographic continuity with the calcite substrate irrespective of the bacterial type (Fig. 3). Two types of precipitates with contrasting sizes and abundances (degrees of surface coverage) were observed: (i) scattered micrometer-sized structures, typically showing a bulgy ellipsoidal or rhombohedral shape, with the latter displaying a preferential orientation (Fig. 3a, c, and e), and (ii) submicrometer-sized rhombohedral crystals blanketing the whole surface of the calcite single-crystal substrate (i.e., 100% surface coverage), showing a very well defined preferred crystallographic orientation (Fig. 3b, d, and f). The micrometer size of the bulgy precipitates and their variable, yet predominantly elongated (rod-like) shapes suggest that they correspond to calcified bacterial cells attached to the substrate. In contrast, the abundant smaller crystals correspond to calcium carbonate crystals directly precipitated on the substrate. The surface density of the larger precipitates (i.e., calcified bacterial cells attached to the substrate) followed the sequence *B. diminuta* (3×10^7 calcified cells/cm^2)–*M. xanthus* (1.5×10^7 calcified cells/cm^2)–bacterial community (0.8×10^7 calcified cells/cm^2). These values are very similar to the attached cell density values reported by Davis and Lüttge (12) for the attachment of *Shewanella oneidensis* MR1 to calcite {10 $\bar{1}$ 4} faces (0.3×10^7 cells/cm^2 after 35 h of culturing). The lower surface cell density values on samples studied by AFM than on samples with *M. xanthus* observed by FESEM are explained by the shorter culture time in the former case (24 h or 48 h versus 7 days). Some differences in the morphology of the smaller precipitates were observed. Samples subjected to mineralization in the presence of the bacterial community or *M. xanthus* displayed a blanket of ca. 0.5-μm "saddle-like" crystals (Fig. 3d) or tear-shaped rhombohedra (Fig. 3f), respectively. In general, bacterial carbonates showed a preferred crystallographic alignment with the <$\bar{4}$ 41> directions of the calcite {10 $\bar{1}$ 4} cleavage face (62). Note that the <$\bar{4}$ 41> directions correspond to two of the periodic bond chains (PBC) present in the calcite cleavage faces (35). As such, these directions are parallel to the acute and obtuse steps observed during the growth and dissolution of calcite cleavage planes (e.g., 71,

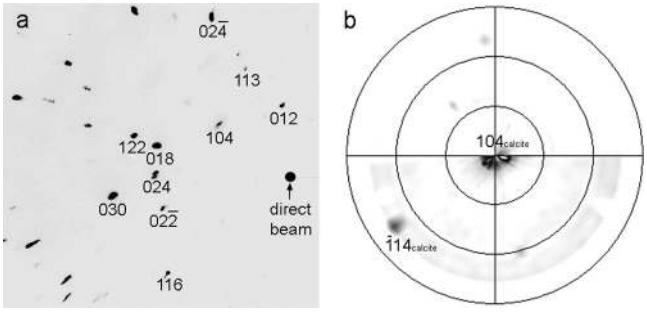

FIG 2 2D-XRD pattern of bacterial calcite formed on the cleavage face of a calcite single crystal (a) and the corresponding pole figure (b). A preferred orientation of bacterial calcite with the [104] pole parallel to the [104] pole of the calcite support is observed. The main Bragg peaks of calcite in panel a are indicated. Note the absence of Debye rings in panel a, which confirms the preferred crystallographic orientation of bacterial calcite.

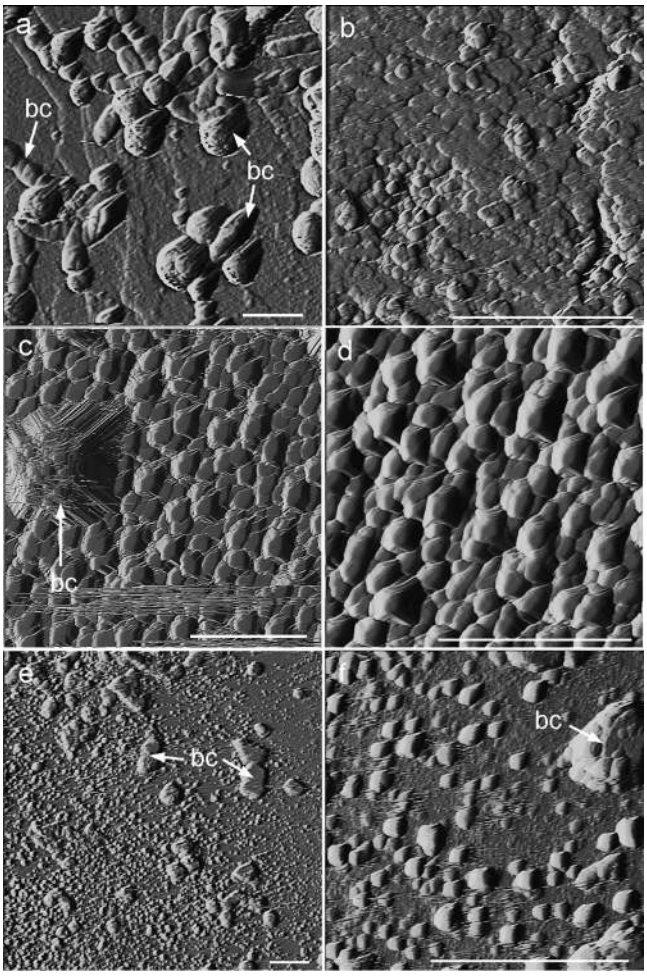

FIG 3 AFM deflection images (taken in air) of bacterial calcite precipitates formed on calcite single crystals. (a) Calcified *B. diminuta* cells (calcified bacterial cells [bc]); (b) detail of oriented calcite overgrowth formed in the presence of *B. diminuta*; (c) precipitates (growth islands) formed in the presence of the bacterial community, including a micrometer-sized growth structure associated with a calcified bacterial cell; (d) detail of oriented calcite growth islands formed in the presence of the bacterial community; (e) precipitates formed in the presence of *M. xanthus*, including micrometer-sized calcified bacterial cells and 2D nuclei; (f) detail of 2D nuclei (growth islands) formed in the presence of *M. xanthus*. Bars, 2 μm.

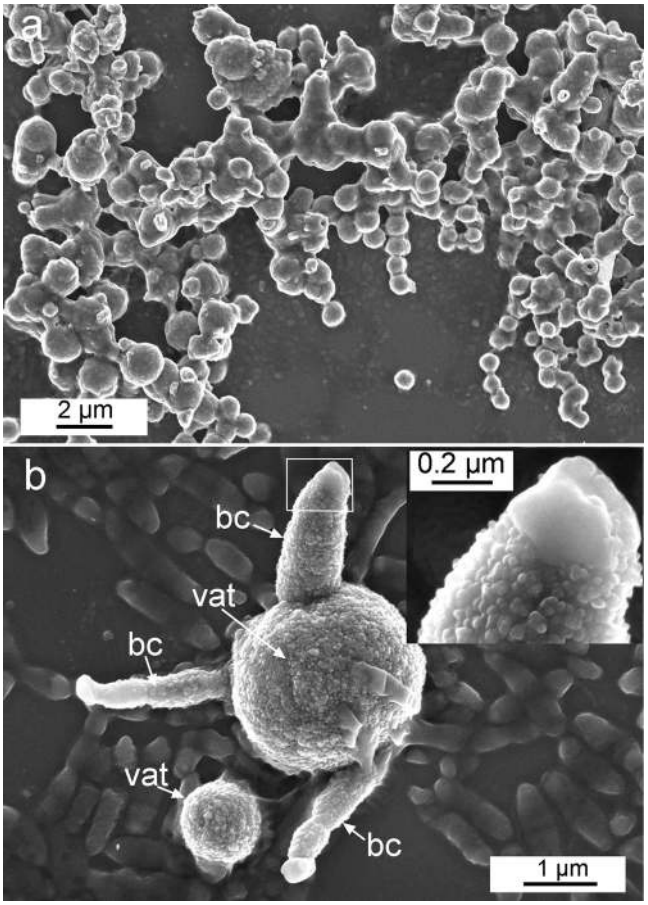

FIG 4 FESEM images of vaterite structures formed in the presence of *B. diminuta* on glass coverslips. (a) General view of vaterite spheres linked by EPS. Bacterial casts (arrows) are observed. (b) Vaterite spheres (vat) showing partially calcified *B. diminuta* cells ([bc]) and uncalcified bacterial cells attached to the substratum. (Inset) Detail of a partially calcified cell covered by nanometer-sized spherical precipitates (diameter, ca. 30 nm).

72). The preferred orientation and (nearly) rhombohedral shape of bacterial precipitates observed on the calcite substrate is consistent with the formation of calcite in all cases, as demonstrated by XRD analyses.

In contrast, only vaterite formed on the surfaces of glass coverslips cultured for 7 days in the presence of *B. diminuta* or the bacterial community, as confirmed by XRD analyses. No precipitates were detected on the control samples, while the amount of precipitates formed on samples cultured in the presence of *M. xanthus* was negligible. Bacterial vaterite appeared as scattered micrometer-sized spheres (diameter, ca. 1 to 2 μm) attached to the silicate substrate (Fig. 4a). Surface coverage by vaterite spheres was highest (30%) in the presence of *B. diminuta*. Some randomly oriented bacterial cells, apparently not calcified (as shown by their very low contrast and higher gray level), were observed attached to the glass substrate cultured with the bacterial community or *B. diminuta* (Fig. 4b). The surface cell density ranged from $(2.5 \pm 1) \times 10^7$ cells/cm^2 (bacterial community) to $(1.6 \pm 1) \times 10^8$ cells/cm^2 (*B. diminuta*). These values are 1 to 2 orders of magnitude smaller than that for *M. xanthus* on the calcite substrate following a culture time of 7 days (FESEM observations). They are, however, very similar to those reported by Fletcher and Loeb (26) for surface attachment of a marine *Pseudomonas* sp. to glass [$(0.8 \pm 0.2) \times 10^8$ cells/cm^2)]. Some bacterial vaterite structures displayed a core-shell structure (Fig. 4a, arrows), similar to that described elsewhere (11, 70). The inset in Fig. 4b shows a detail of a partially calcified *B. diminuta* cell. The rod-shaped cell is surrounded by an aggregate of (nearly) spherical nanocrystals of 34 ± 10 nm. However, the edge of the cell is not calcified. The size and morphology of the nanoparticles mentioned above are strikingly similar to that of ACC formed as a precursor of crystalline calcium carbonate (64). Vaterite precipitates were surrounded by a significant amount of EPS, which formed a nearly continuous film. In contrast to the case of the calcite substrate, no apparent preferential orientation of the bacterial vaterite precipitates was observed. Unfortunately, 2D-XRD analyses failed to confirm the absence of any preferred crystallographic orientation of vaterite due to the low crystallinity and limited coverage density of such precipitates,

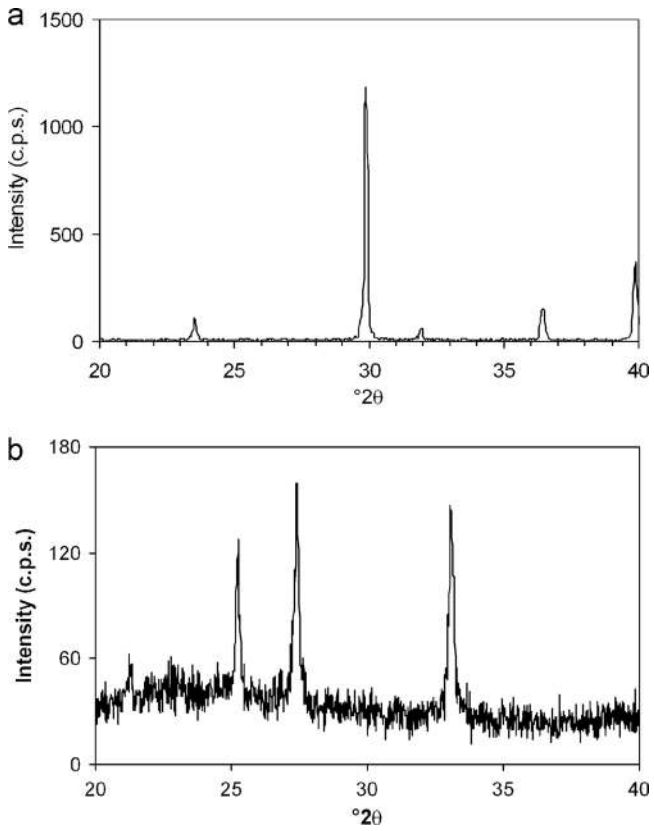

FIG 5 XRD patterns of bacterial calcium carbonates formed on marble and porous glass supports. (a) Calcite on marble; (b) vaterite on porous glass.

which resulted in very diffuse (poorly defined) 2D diffraction patterns.

Bacterial mineralization on marble and porous sintered glass. In agreement with the results presented above, calcite formed on the calcitic marble while vaterite formed on the porous glass support, as shown by XRD analyses (Fig. 5). Figure 6 shows FESEM images of precipitates formed on these two substrate types subjected to mineralization in the presence of *M. xanthus*. Compact aggregates of oriented calcite crystals grew on the calcite grains of the marble (Fig. 6a and b). Vaterite appeared as dense aggregates of micrometer-sized spheres (diameter, ca. 2 to 6 μm) covered by an EPS film (Fig. 6c and d). As with the vaterite spheres formed on glass coverslips, the surfaces of these precipitates were very rough due to the presence of aggregates of nanometer-sized building blocks similar to those reported elsewhere (70).

Bacterial mineralization on calcarenite and sandstone. SEM analyses showed the development of bacterial biofilms with mineralized bacterial cells and EPS on the surfaces and in the intergranular spaces of the microsparitic calcite cement of calcarenite (Fig. 7a). Nearly 100% coverage of the calcite grains by bacterial calcite (identified by its rhombohedral shape) was observed. The presence of mineralized bacteria was observed down to a depth of 3 cm (the full thickness of treated stone slabs) (Fig. 7b). The density of calcified bacterial cells attached to the calcite substrate was $(1 \pm 0.2) \times 10^7$ cells/cm^2. No vaterite was detected by XRD.

For the treated sandstone, XRD analyses of depth profiles showed that calcium carbonate precipitated as vaterite down to a depth of 8 to 9 mm. SEM observations revealed that quartz grains in the sandstone were covered with mineralized bacterial EPS and numerous micrometer-sized spherulites of vaterite in contact with mineralized bacterial cells down to a depth of 15 mm (that is, the full thickness of treated stone slabs) (Fig. 7c and d). The density of calcified bacterial cells attached to the quartz grains was $(1 \pm 0.1) \times 10^6$ cells/cm^2, a value 1 order of magnitude lower than that determined for the calcitic stone. In any case, surface cell densities on the carbonate and silicate stones were, respectively, ca. 1 order of magnitude lower than those observed after bacterial treatment of calcite single crystals and glass coverslips for 7 days.

DISCUSSION

Bacterial carbonatogenesis. All bacteria tested induce the precipitation of a significant amount of calcium carbonate when cultured in M-3P medium. This was not unexpected. The formation of calcium carbonate in such a medium has been reported for *M. xanthus* (4, 69, 70) and *B. diminuta* (40), as well as for the bacterial community inhabiting weathered calcarenite stones (38, 40) and undecayed quarry calcarenite stones (39). Studies performed since the beginning of the 20th century demonstrate that numerous heterotrophic bacteria induce the precipitation of calcium carbonate in a range of natural environments and laboratory culturing conditions (references 31 and 69 and references therein). Urzi et al. (86) showed that bacteria isolated from a range of building stones exposed to different environments are, in most cases, carbonatogenic. These observations emphasize the fact that bacterial carbonatogenesis is a common and widespread phenomenon, which can take place in a range of environments, including building stones. Various bacterial metabolic activities, such as carbon dioxide fixation, nitrate reduction, or oxidative deamination of amino acids, can induce calcium carbonate precipitation (16, 31). This is brought about by locally changing the physicochemical parameters, e.g., increasing the pH and the total dissolved inorganic carbon (DIC) content in the environment in which bacteria live (69). The metabolic activity of *M. xanthus*, as well as that of most heterotrophic bacteria isolated from carbonate building stones, such as *B. diminuta*, results in the production of ammonia by means of oxidative deamination of amino acids. Ammonia creates an alkaline microenvironment around the bacterial cell consistent with the thoroughly observed pH rise that takes place during the initial stages of bacterial carbonatogenesis (21, 38, 69, 70). The main source of CO_2 is atmospheric, but this gas is also produced by bacterial activity. In solution, it transforms into HCO_3^- or CO_3^{2-} as the pH increases, thus contributing to an increase in carbonate alkalinity. Calcium ions can be supplied by the culture medium or may result from the dissolution of the support (e.g., limestone) to which bacteria are attached. In turn, calcium ions can be adsorbed on the negatively charged bacterial cell walls (6, 83) and EPS (60), increasing the calcium concentration locally. As a result, local supersaturation with respect to either vaterite or calcite is reached in the surrounding of the bacterial cells or at the bacterial cells, as well as within bacterial biofilms. Once sufficient supersaturation is achieved, calcium carbonate formation by heterogeneous nucleation can readily occur on the bacterial cell walls and bacterial EPS or cell debris, as well as on the mineral substrate (i.e., calcite or glass/quartz). The former effects occur on both carbonate and silicate substrates, leading to cell entombment and EPS calcification. Conversely, heterogeneous nucleation on the substrate is most effective on calcite substrates. This effect results in the

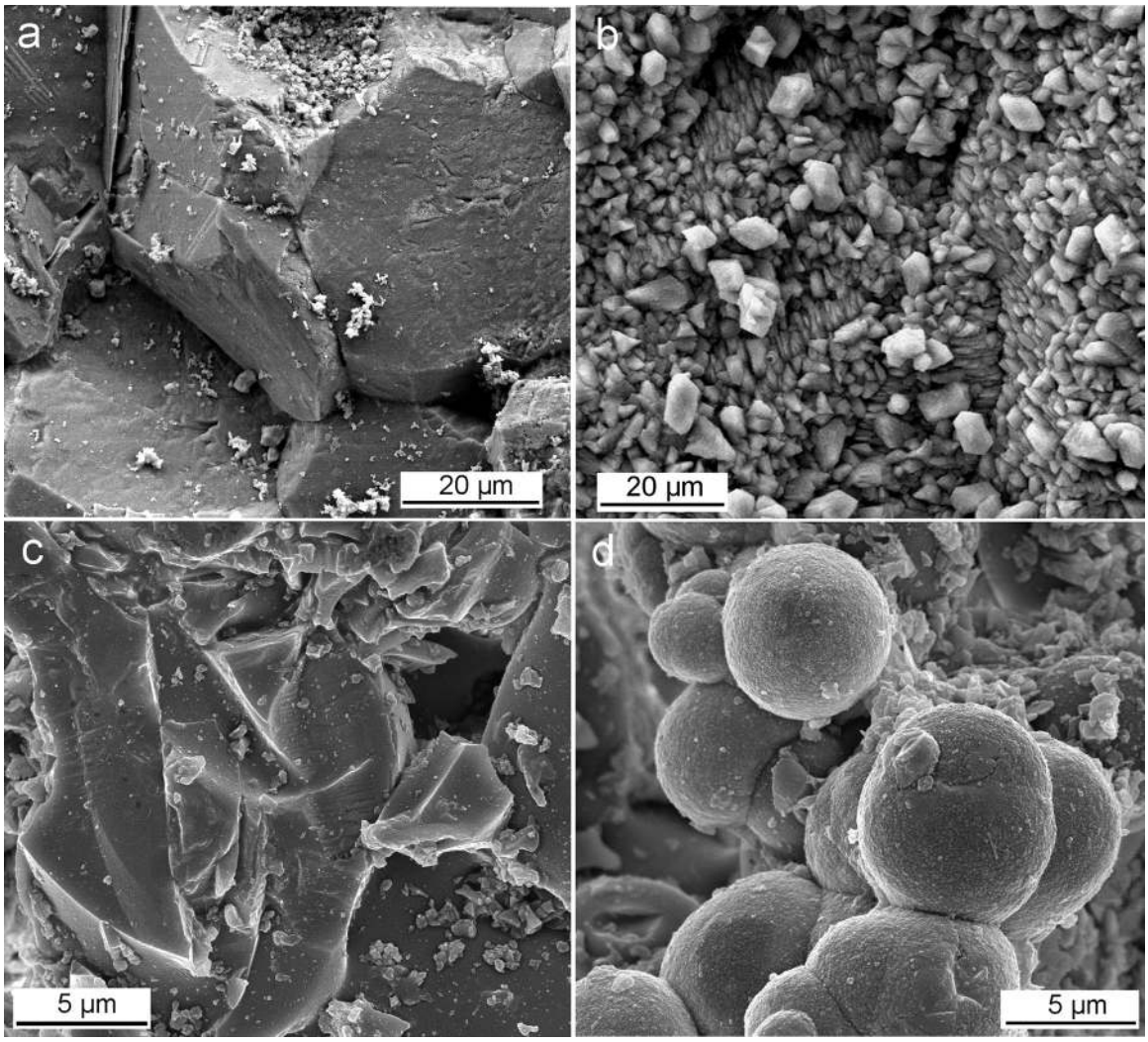

FIG 6 FESEM images of calcium carbonate precipitates formed on marble and porous glass substrates treated with *M. xanthus* for 28 days. (a and b) Marble surface before (a) and after (b) the formation of oriented bacterial calcite. (c and d) Porous glass support before (c) and after (d) the formation of aggregates of spheroidal vaterite linked by EPS.

epitaxial growth of bacterial calcite crystals displaying the observed preferred crystallographic orientation, which matches that of the calcite crystals in the substrate.

The saturation index (SI) [$SI = \log \Omega = \log (IAP/K_s)$, where Ω is the saturation state of the system, IAP is the ion activity product, and K_s is the thermodynamic solubility product of the relevant phase] of M-3P medium with respect to calcium carbonate phases, was calculated using PHREEQC computer code (63). The results show that this culture medium is supersaturated with respect to calcite (SI, 2.16), aragonite (SI, 2.01), and vaterite (SI, 1.54). Considering that calcium carbonate in microbial systems is typically precipitated when the saturation index (with respect to calcite) is above 1 (2, 58), one should expect the (spontaneous) precipitation of any of the three calcium carbonate polymorphs in biotic experiments. Moreover, calcite should grow readily on the calcitic substrate (control) via heterogeneous crystallization (self-epitaxy, or homoepitaxy). However, no precipitation is observed in the control runs for either carbonate or silicate substrates. In fact, instead of the expected growth, a general dissolution of the calcitic substrate is observed. This can be explained by the presence of Bacto Casitone in M-3P medium. Bacto Casitone is made up of hydrolyzed proteins that display a large number of functional groups (carboxylic and amino groups) (70). Molecules with such functional groups can form Ca complexes, i.e., they have a chelating action (27), thereby reducing the Ca activity in the liquid medium to a level where the SI with respect to calcite becomes negative. As a result of such undersaturation, the observed dissolution of the substrate occurs. Furthermore, these organics can play a role as crystallization inhibitors (when in solution), thus preventing the nucleation of calcium carbonate even at SI values as high as those initially present in M-3P medium (70).

It follows that bacterial presence and activity are a prerequisite for the precipitation of calcium carbonate. Bacterial metabolic activity produces the increase in supersaturation necessary to induce the heterogeneous crystallization of calcium carbonate both on the support (in the case of the calcitic support) and on the surfaces of bacterial cells attached to the solid substrate, as well as on EPS (in the case of both the calcitic and silicate substrates).

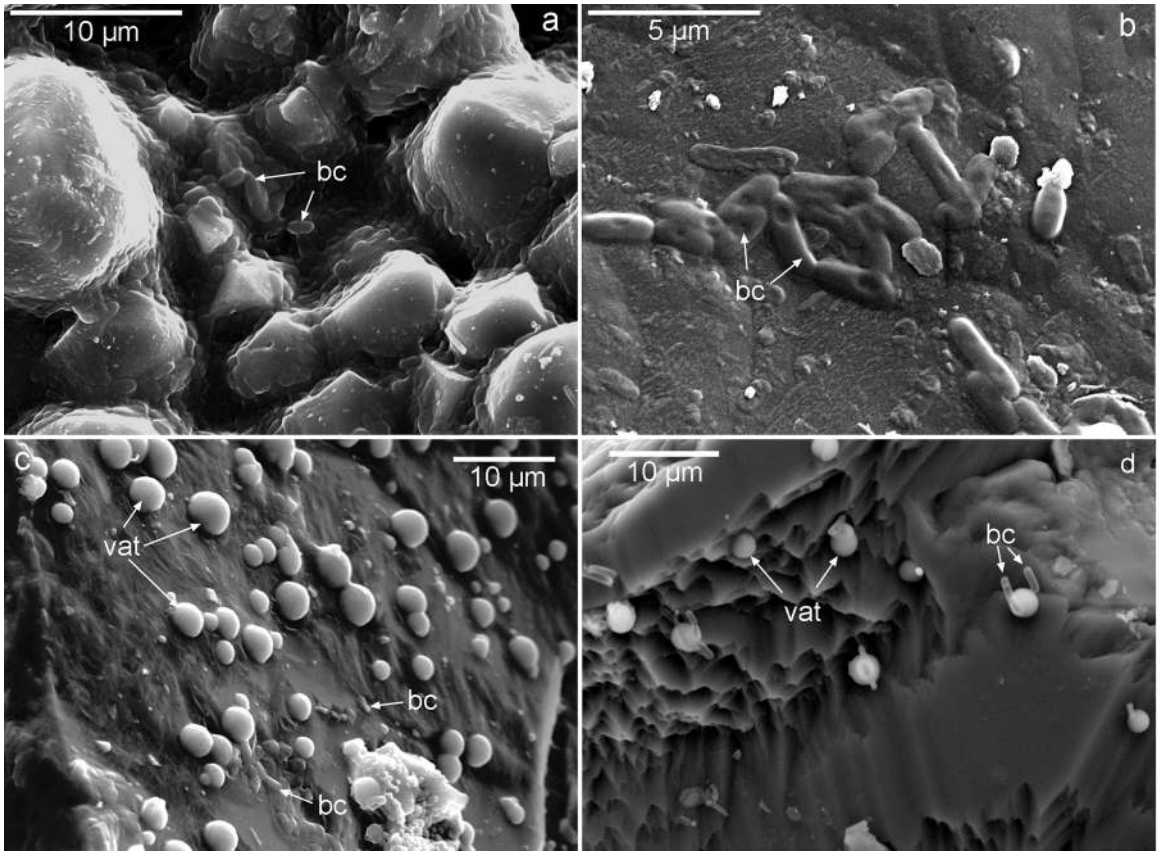

FIG 7 SEM images of treated carbonate and silicate stones. (a) Newly formed bacterial calcite along with calcified bacterial cells (bc) embedded in EPS on the calcarenite stone. (b) Detail of calcified bacterial cells attached to the calcite grains in the calcarenite stone. (c) Vaterite spheroidal precipitates (vat) on the quartz grains of the sandstone, along with a few bacterial cells embedded in EPS. (d) Bacterial cells partially entombed in vaterite spherulitic precipitates attached to quartz crystals.

Roles of substrate composition and structure in bacterial $CaCO_3$ polymorph selection. Our results show that the presence of a calcitic substrate promotes the epitaxial growth of bacterial calcite. Conversely, spherulitic vaterite forms on the silicate substrate. This occurs systematically regardless of the bacterial type and/or the texture/porosity of the substrates. These results demonstrate that, at least in the systems studied, polymorph selection in bacterial calcium carbonate mineralization by heterotrophic bacteria is not bacterium or strain specific. Rather, under equal culture conditions, the nature of the substrate strongly influences which polymorph is formed.

In the absence of additives or impurities, the phase, amount, and morphology of calcium carbonate minerals formed in solution depend on the SI (supersaturation), temperature, pH, and $[Ca^{2+}]/[CO_3^{2-}]$ ratio. Under conditions far from equilibrium (i.e., high supersaturation), where kinetics rather than thermodynamics control crystallization (43), the crystallization of $CaCO_3$ typically follows the Ostwald step rule (57, 61). This rule dictates that the crystallization of the less stable (more soluble) phase(s) will precede that of the more stable phase(s). For calcium carbonate, the crystallization sequence according to the Ostwald rule is as follows: ACC, vaterite, aragonite (temperature, >30 to 35°C), calcite (57, 61, 67). At room temperature and an alkaline pH (8.5 to 10.5), the formation of vaterite is favored (82). This phase typically appears as spherulites made up of radial fibrous crystals elongated along their *c* axis (70). Vaterite may eventually transform into stable calcite via a dissolution/precipitation process (79). Conversely, at room temperature and a pH close to neutrality, as well as at pH >11, the development of calcite is promoted (82). The presence of organic additives and/or foreign ions, such as Sr and Mg, can strongly affect polymorph selection (51). Organics (e.g., soluble proteins) can play different roles during biomineralization, either as complexation agents and crystallization inhibitors when in solution or as the templates for nucleation when adsorbed onto a substrate (1). Organics in solution (DOC), acting as kinetic inhibitors, tend to induce the precipitation and stabilization of vaterite (70).

In our experiments using calcitic substrates, heterogeneous nucleation of bacterial calcite occurs on the existing calcite crystals. In this respect, the formation of calcite (easily identified by its rhombohedral morphology) during bacterial conservation of calcitic stones is typically reported (16, 19, 38, 39, 69, 84). Because the substrate facilitates the direct crystallization of stable calcite at relatively low supersaturation, the Ostwald rule does not apply despite the abundance of organics that could act as kinetic inhibitors. In this case, the crystallization is homoepitactic. Homoepitaxy (or self-epitaxy) has been described in a number of systems and has found numerous technical applications (10). The crystallographically coherent boundary between the substrate and the newly formed homoepitaxial precipitate ensures good adhesion.

This is critical in a consolidation or protection treatment of stone (69).

Interestingly, our AFM observations show two types of oriented calcite precipitates on the calcite single-crystal substrate. The larger (micrometer-sized), scattered growth structures display features that could correspond to growth hillocks associated with emerging dislocations (72). However, despite the fact that in many cases these precipitates are well aligned with the $<\bar{4}\ 41>$ directions, in a few cases they are not. In addition, they typically have an elongated, rod-like or ellipsoidal (sometimes curved) shape (Fig. 3a). These observations indicate that these structures correspond to calcified bacterial cells that have attached to the surface, as the AFM study of *B. pasteurii* $CaCO_3$ production by Warren et al. has shown (87). Once attached, bacterial cells can adsorb Ca ions (6), thus creating the local physicochemical conditions to foster the formation of calcite entombing the cells (83). Upon entombment of such bacterial cells, further growth of calcite along $<\bar{4}\ 41>$ directions leads to the observed preferred orientation of the micrometer-sized rhombohedral structures.

The smaller crystals observed by AFM appear to correspond to homoepitaxial calcite grown according to classical crystallization theory. That is, the precipitates form by 2D nucleation of growth islands on the surface of the calcite cleavage face at a relatively high supersaturation (57). However, the morphology of such calcite overgrowths does not always match that of the typical rhombohedral growth islands (i.e., "saddle-like" or tear-shaped). The observed nanoscale morphological modifications are, however, consistent with calcite growth in the presence of abundant biomolecules (18). As stated above, the culture medium includes several organic molecules, and bacterial activity results in the production of EPS, which includes polysaccharides and soluble proteins. These organics in solution (i.e., DOC) can interact with (adsorb onto) specific growth steps of the 2D islands, thereby modifying their morphology (18). Ultimately, such organics can be incorporated into the biominerals as growth progresses. Incorporation of organics within bacterial vaterite has been demonstrated by Rodriguez-Navarro et al. (70), while histological and fluorescence microscopy of stained bacterial biominerals has demonstrated the incorporation of EPS into vaterite and calcite (94). Incorporation of organics is a general phenomenon during calcium carbonate biomineralization and biomimetic crystallization (48), and it has profound effects not only on the morphology of precipitates but also on the physicochemical properties of such hybrid organic-inorganic structures (1). Rodriguez-Navarro et al. (69) argued that the higher resistance to dissolution and mechanical stress (sonication) of bacterial calcite is consistent with the incorporation of organics into this biomineral.

In contrast, the silicate substrates tested (both amorphous [glass] and crystalline [quartz]) do not present any chemical or structural/crystallographic similitude with any crystalline calcium carbonate phase. Therefore, no epitaxial growth should be expected, as shown by Lioliou et al. (50), who observed homogeneous nucleation of abiotic calcium carbonate at very high supersaturation in the presence of quartz crystals (i.e., the silicate substrate did not induce heterogeneous nucleation). For the silicate substrates tested here, there is also no "template" that may help minimize the energy requirements to foster heterogeneous nucleation. Therefore, a significant departure from equilibrium (i.e., high supersaturation) occurs, and kinetics, rather than thermodynamics, control the crystallization of bacterial calcium carbonate. To such an absence of a matching substrate, one must add the crystallization inhibition brought about by the organics in the system. Due to such a high departure from equilibrium, the Ostwald rule of stages is at work, enabling the formation of metastable phases such as vaterite. It has been shown that *M. xanthus* is able to induce the formation of vaterite due to kinetic inhibition induced by organics (70). Such organics, which are incorporated into bacterial vaterite, prevent its rapid transformation into stable calcite. Our FESEM observations of aggregates made up of nanometer-sized spheres, ca. 30 nm in diameter, covering bacterial cells during the early stages of calcification suggest that the formation of ACC precedes that of bacterial vaterite, as reported by Chen et al. (11). Note that ACC typically appears as spheres of ca. 30 nm, with a proposed upper size limit of ca. 120 nm; conversely, crystalline calcium carbonates are reported to be stable above 70 nm (64). The observed nanometer-sized building blocks that formed around bacterial cells during the early stages of mineralization, as well as those that formed on the rough surfaces of spheroidal $CaCO_3$ structures after 7 days and 28 days of culture on glass coverslips and porous glass, respectively, are typical in vaterite mesocrystals, and this primary tecton unit size reportedly corresponds to the size of amorphous precursor nanoparticles (57). Our observations suggest that ACC formed and, following aggregation on the bacterial cell surface, transformed into vaterite in accordance with the Ostwald step rule. The fact that the typical pH during bacterial carbonatogenesis of vaterite ranges between 8 and 9.5 (69, 70) is consistent with recent results indicating that under mild alkaline conditions (pH 8.5 to 9.5), ACC with a protovaterite structure develops and eventually transforms into such a phase (28). All in all, our observations, as well as the results published in the literature cited, point out that the formation of bacterial vaterite on the silicate substrates is due to kinetic effects and follows the Ostwald rule.

While in our experiments there is a direct relationship between substrate type and calcite or vaterite precipitation, the relationship is not always that straightforward. Rodriguez-Navarro et al. (69) reported the formation of bacterial vaterite on a calcitic support when *M. xanthus* was cultured in M-3 medium. This medium is similar to M-3P medium but lacks a phosphate buffer. The absence of such a buffer leads to a higher pH during bacterial mineralization. The high pH and the subsequent increase in SI values help explain why vaterite is kinetically favored in this system even though a calcitic substrate is present. De Muynck et al. (17) showed the formation of (oriented) bacterial calcite rhombohedra on limestone when a urea-rich *Bacillus sphaericus* culture was dosed with Ca as $CaCl_2$. Conversely, the use of calcium acetate as a Ca source led to the precipitation of calcium carbonate with a disk-shaped morphology typical of vaterite. The authors observed similar effects in the case of calcium carbonate precipitation on concrete mediated by the same ureolytic bacteria (15). Although they provided no explanation for the change in the morphology (and phase) of bacterial precipitates, it could be argued that acetate ions, acting as an additional carbonyl carbon source (93), can lead to higher bacterial activity, EPS production, and supersaturation. High supersaturation and abundant organics may, in turn, kinetically favor vaterite precipitation, as discussed above. Note that enhanced production of EPS typically occurs under an excess of carbon over nitrogen sources (90). Therefore, the observed substrate effect on polymorph selection of bacterial calcium carbo-

nates may be overruled by enhanced bacterial activity and EPS production, with the resulting high departure from equilibrium, which kinetically favors vaterite formation. This is in good agreement with a study by Kim et al. (42) on the polymorph selection of $CaCO_3$ through epitaxy with inorganic substrates. The authors showed that abiotic epitaxial selection of the calcium carbonate polymorph by the substrate occurred only below a threshold supersaturation.

On the other hand, precipitation of calcite on quartz sand grains following a biocementation treatment with ureolytic bacteria has been reported (14, 29, 80). Because the silicate substrate does not induce the heterogeneous (epitaxial) crystallization of calcite, thereby leading to high supersaturation, the Ostwald rule will be at work. Under these physicochemical conditions, vaterite will form as a precursor of calcite and eventually will transform into stable calcite, as shown by Chen et al. (11) also for ureolytic bacteria. Unlike the vaterite structures formed in the presence of bacteria in this study or in that of Rodriguez-Navarro et al. (70), vaterite produced by ureolytic bacteria does not seem to incorporate sufficient organics to prevent its dissolution-mediated transformation into stable calcite. This may explain why bacterial calcite can eventually form on quartz grains. This rationale may also help to explain why different carbonatogenic bacteria cultured in glass flasks (with the same growth medium) produce either vaterite or calcite plus vaterite (76).

Bacterial attachment to substrates. The different capacities of bacteria to attach to different mineral substrates may help explain the observed differences in bacterial carbonate productivity on calcitic and silicate substrates. Attachment of bacteria to mineral surfaces is a ubiquitous process in natural environments and in the laboratory (12, 26, 37, 52, 54, 75). It can be detrimental (e.g., biocorrosion or biofouling) or beneficial, for instance, when bacterial mineralization is the target process (16). Attachment occurs in four distinct steps: (i) transport to the mineral surface, (ii) initial adsorption (or adhesion), (iii) attachment via EPS or fibril formation, and (iv) colonization (i.e., formation of a biofilm) (55). Adhesion is driven mainly by interfacial energy reduction via hydrophilic and/or hydrophobic bacterium-substrate interactions (26). Bacterial attachment to hydrophilic mineral surfaces in contact with a solution, where a surface charge exists, is driven mainly by electrostatic interactions (75). Hydrophobic or steric interactions contribute strongly to bacterial adhesion, especially for organic substrates such as polystyrene, Teflon, or epoxy (26, 52, 75).

At the alkaline pH reached during bacterial carbonatogenesis (i.e., pH 7.5 to 9.5) (38), bacterial cells will have a net negative charge (6, 34, 75). The glass and quartz silicate substrates also have a negative charge, because their pH at zero point of charge (pH_{ZPC}) is ca. 2.0 (81). Conversely, calcite either will have no net charge or the surface charge will be slightly positive, because the calcite pH_{ZPC} is 8.0 to 9.5 (77). Electrostatic interactions will dominate bacterium-mineral adhesion in our systems, since both calcite and quartz/glass are hydrophilic (i.e., the solution/mineral contact angle is $<90°$) and the ionic strength of M-3P culture medium is relatively low, thus limiting screening effects (75). More-efficient attachment, at a higher rate, is therefore expected for the calcitic substrate, where attractive forces would easily outweigh repulsion forces (75). This explains why a greater number of attached bacterial cells are observed on calcite single-crystal surfaces. In this respect, Dick et al. (19) report that one key parameter for bacterial carbonate biodeposition on limestone is the ξ potential of bacteria (i.e., the net surface charge of the bacterial cells determined using electrokinetic measurements). Bacteria with a higher negative ξ potential are more easily retained by the positively charged surface of calcite, thus favoring adhesion and surface colonization and ultimately leading to good limestone restoration (16). In contrast, bacterial attachment to glass or quartz surfaces under the physicochemical conditions of our experiments is limited, as reflected by the lower surface density of bacterial cells. Our results are consistent with those of Scholl et al. (75), who observed a higher degree of attachment of bacterial cells to limestone chips than to quartz chips. They also agree with those of Ferris et al. (25), who found a 10-fold to 100-fold lower adsorption of bacterial cells on silicate surfaces (including quartz) than on calcite. Bosak and Newman (8) showed that carbonate-producing *Desulfovibrio desulfuricans* cells have a strong preference for attaching to calcite crystals rather than to glass. Very weak bacterial cell adsorption on quartz at circumneutral pHs has been reported by Hendricks (36), Fletcher and Loeb (26), and Yee et al. (92). Interestingly, AFM and vertical scanning interferometry (VSI) observations of calcite-microbe interactions show that *S. oneidensis* MR-1 cells are entrenched in biotically formed pits ca. 130 nm deep (12). Such an entrenchment mode, which is probably much more difficult to achieve in less soluble silicates, may contribute to favoring the adhesion of bacterial cells to calcite substrates.

It has been reported that bacterial attachment to solid substrates has a significant impact on bacterial resistance to physicochemical stressors (93) and enhances bacterial metabolic activity and growth (36, 52). Manini and Luna (55) reported that bacterial heterotrophic production is enhanced in calcite microcosms and is reduced in quartz microcosms by using marine bacteria. This enhanced bacterial activity, along with the larger amount of bacterial cells attached to the calcitic substrates, may help explain why here larger amounts of calcium carbonate (calcite) are systematically observed to be precipitated on calcitic substrates, regardless of the bacterial type and/or the textural features of these substrates. Lower attachment efficiency, and the resulting limited bacterial activity, explains why limited production of calcium carbonate (vaterite) is observed on silicate substrates.

Surface roughness also plays a role in bacterial attachment (55, 75). This may help explain why even in the case of a silica surface, significant attachment resulting in abundant bacterial mineralization of vaterite is observed in the porous glass support as well as in the porous sandstone. Such bacterial precipitates are more abundant than on the flat surface of the glass coverslip. However, no direct comparison between these tests is possible, because of their different durations (i.e., 7 days for of the glass coverslips and 28 days for the porous glass) and treatment conditions (i.e., culturing in inoculated test tubes versus direct spraying of the sterile culture medium onto stone blocks). For the calcitic substrate, it is difficult to evaluate to what extent surface roughness plays a role in bacterial attachment and carbonate productivity. Nonetheless, in all cases, from the atomically flat surface of calcite single crystals or the nearly flat surface of marble to the very rough pore surface of the calcarenite stone, nearly 100% surface coverage is systematically achieved (despite differences in bacterial type and test duration).

Implications for stone conservation. The results of this study have direct implications for the conservation of the built heritage

and statuary made of stone. They show that structurally and mechanically coherent, and therefore durable, bacterial calcite cement is abundantly formed when a bacterial treatment is applied to calcitic stones such as limestone and marble. In this case, calcite is formed homoepitaxially. The newly formed calcite overgrowth is produced by specific heterotrophic carbonatogenic bacteria, such as *M. xanthus* or *B. diminuta*, as well as by the carbonatogenic bacterial community isolated from decayed building stones. Furthermore, such an abundant bacterial calcitic cement is produced *in situ* following the application of a sterile nutritional solution to a decayed ornamental limestone that contains its own microbiota. The latter represents the actual scenario for an *in situ* application of a bacterial treatment according to the patent held by Gonzalez-Muñoz et al. (30). Interestingly, this treatment is effective to a depth of several centimeters, fully ensuring an effective conservation treatment (20). Such a significant depth of penetration may be associated with two phenomena: (i) irrespective of their position in a depth profile, bacteria inhabiting the calcitic stone are activated as soon as the nutritional medium reaches their location; (ii) activated bacteria are transported in suspension (in the culture medium) through the porous stone system.

In contrast, limited amounts of spherulitic vaterite are formed on silicate supports (glass and quartz sandstone). The depth of penetration of the bacterial carbonatogenic treatment on sandstone is also on the centimeter scale, which may favor deep consolidation in actual on-site applications. In this respect, it should be noted that under static conditions, the motility and growth of bacteria have been found to result in transport rates as high as 0.4 cm h^{-1} in nutrient-saturated sand and sandstone (reference 75 and references therein). However, such vaterite precipitates do not attach coherently to the substrate, since they display significant structural (crystallographic) mismatching. This may limit the formation of a mechanically resistant bacterial cement binding mineral grains of silicate stones in an actual conservation application of the bacterial treatment. Although this might be a handicap for the efficiency of the treatment, it does not invalidate it. It is expected that bacterial vaterite, which is metastable, will eventually dissolve and be reprecipitated as calcite (79). Such a dissolution/precipitation phase transition may lead to the formation of a more (chemically and mechanically) resistant calcium carbonate cement following application of the bacterial treatment to silicate stones. Note that it has been shown that effective consolidation of loose sand and sandstones can be achieved following calcium carbonate production by ureolytic bacteria (14, 24, 80, 89). However, ureolytic bacteria do not seem to be abundant on weathered building stones (40, 86).

Another issue to be considered is that under conditions far from equilibrium (e.g., very high pH) favoring a high SI, kinetic effects may lead to the precipitation of bacterial vaterite on a calcitic substrate, an undesired effect that could be bypassed by the proper selection of the culture medium (e.g., M-3 versus M-3P) (69). Conversely, bacterial cultures that produce limited amounts of organics, thereby favoring the rapid (on a scale of days) transformation of vaterite into calcite, could be selected for the consolidation of sandstones (e.g., *B. subtilis* or *A. aerogenes*) (11). This, however, prevents one from taking advantage of the benefits (in terms of ease of treatment preparation and application, as well as reduced cost) of the application of a sterile nutritional solution to induce the activation of carbonatogenic bacteria present in decayed stones. In any case, the lack of a chemical and structural similarity between either vaterite or calcite and a silicate (quartz) substrate remains an issue that should be addressed. Note that such a mismatch has been recognized as a significant limitation in the conservation of limestone using ethyl silicates, because the resulting silica gel cement does not coherently bind to calcite (20). A possible solution for this problem is the use of a coupling agent with an anchor group on one end that binds to calcitic grains and a hydroxyl group on the other end that binds to silica gel (74). The same approach could be applied to the bacterial conservation of silicate stones.

This discussion applies to other technical processes where bacterial carbonatogenesis plays a role, such as the strengthening of sand and soil, which should be much more effective for carbonate than for silicate (quartz) sand and soil. In the application of a bacterial treatment to cement structures, the production of calcite following the carbonation of portlandite [$Ca(OH)_2$], which typically accounts for 10 to 25% (by weight) of the phases formed upon cement hydration, ensures that bacterial calcite will typically form, as observed by De Muynck et al. (15).

Conclusions. We have shown that bacterial calcium carbonate polymorph selection is not bacterium or strain specific. We have also shown that the substrate type (composition and mineralogy) is critical for polymorph selection and bacterial carbonate productivity. Calcitic substrates favor bacterial attachment and promote the formation of abundant homoepitactic calcite. Such a newly formed bacterial cement is highly coherent and ensures high physicochemical resistance. In contrast, under the same culture conditions, vaterite spheres formed incoherently on silicate substrates, including glass (nonporous and porous) and sandstone. Because of the lack of chemical and crystallographic matching, bacterial precipitation of calcium carbonate in substrates other than calcite will result in precipitation at high supersaturation according to the Ostwald rule, that is, following the sequence ACC–vaterite–calcite. The final bacterial calcium carbonate polymorph that appears in a particular situation will depend strongly on the amount of DOC from bacterial activity, which would affect the vaterite-to-calcite phase transition. A small amount of DOC favors the final formation of calcite, while a large amount of DOC promotes the kinetic stabilization of vaterite.

The degree of bacterial attachment to silicate substrates is lower than that to calcitic substrates. This results in limited bacterial vaterite production. Application of the sterile M-3P culture medium to decayed limestone (calcarenite) and sandstone results in the activation of the carbonatogenic bacteria inhabiting the stones. This leads to the production of bacterial calcite and vaterite in limestone and sandstone, respectively. These results have important implications for the bacterial conservation of ornamental stones other than carbonate stones and demonstrate that the chemical/crystallographic affinity between the substrate and the bacterial biomineral (i.e., the existence or absence of epitaxy) is important in controlling both calcium carbonate polymorph selection and bacterial calcium carbonate productivity. Finally, the depth of the consolidation achieved is noticeable (centimeter scale) and ensures that a bacterial treatment would be effective for *in situ* consolidation of stone. These results also have implications for other technological applications of bacterial carbonatogenesis, such as sand and soil strengthening, solid capture of groundwater contaminants, stable CO_2 mineral sequestration, and cement repair and consolidation. They may also aid in the better under-

standing of bacterial calcium carbonate phase selection and productivity in nature.

ACKNOWLEDGMENTS

This work was supported by grant RNM 3943 and the research groups BIO 103 and RNM 179 (Junta de Andalucía), the Spanish Government under grant MAT2009-11332, and the EU Initial Training Network DeltaMin (Mechanisms of Mineral Replacement Reactions), grant PITN-GA-2008-215360.

We thank A. Rodriguez-Navarro for help during 2D-XRD analyses and J. Vicente Navarro for help with SEM analyses. Scanning electron microscopy analyses were performed at the Centro de Instrumentación Científica of the University of Granada and the Instituto del Patrimonio Histórico Español. We thank A. Putnis and C. V. Putnis for help during AFM analyses that were performed at the Institut für Mineralogie, Münster Universität. We thank four anonymous referees for helpful comments and suggestions.

REFERENCES

1. **Aizenberg J, Hanson J, Koetzle TF, Weiner S, Addadi L.** 1997. Control of macromolecule distribution within synthetic and biogenic single calcite crystals. J. Am. Chem. Soc. **119**:881–886.
2. **Arp G, Reiner A, Reiner J.** 2001. Photosynthesis-induced biofilm calcification and calcium concentration in Phanerozoic oceans. Science **292**: 1701–1704.
3. **Barabesi C, et al.** 2007. *Bacillus subtilis* gene cluster involved in calcium carbonate biomineralization. J. Bacteriol. **189**:228–235.
4. **Ben Chekroun K, et al.** 2004. Precipitation and growth morphology of calcium carbonate induced by *Myxococcus xanthus*: implications for recognition of bacterial carbonates. J. Sediment. Res. **74**:868–876.
5. **Benzerara K, et al.** 2006. Nanoscale detection of organic signatures in carbonate microbialites. Proc. Natl. Acad. Sci. U. S. A. **103**:9440–9445.
6. **Beveridge TJ.** 1989. Role of cellular design in bacterial metal accumulation and mineralization. Annu. Rev. Microbiol. **43**:147–171.
7. **Boquet E, Boronat A, Ramos-Cormenzana A.** 1973. Production of calcite (calcium carbonate) crystals by soil bacteria is a common phenomenon. Nature **246**:527–529.
8. **Bosak T, Newman DK.** 2005. Microbial kinetic controls on calcite morphology in supersaturated solutions. J. Sediment. Res. **75**:190–199.
9. **Braissant O, Cailleau C, Dupraz C, Verrecchia EP.** 2003. Bacterially induced mineralization of calcium carbonate in terrestrial environments: the role of exopolysaccharides and amino acids. J. Sediment. Res. **73**:485–490.
10. **Chan CA.** 1990. Interface epitaxy and self-epitaxy of metals near room temperature. Phys. Rev. E Cond. Matter **42**:11946–11949.
11. **Chen L, et al.** 2009. Bacteria-mediated synthesis of metal carbonate minerals with unusual morphologies and structures. Cryst. Growth Des. **9**:743–754.
12. **Davis KJ, Lüttge A.** 2005. Quantifying the relationship between microbial attachment and mineral surface dynamics using vertical scanning interferometry (VSI). Am. J. Sci. **305**:727–751.
13. **Decho AW.** 2010. Overview of biopolymer-induced mineralization: what goes on in biofilms? Ecol. Eng. **36**:137–144.
14. **DeJong JT, Fritzges MB, Nüsslein K.** 2006. Microbially induced cementation to control sand response to undrained shear. J. Geotech. Geoenviron. Eng. **132**:1381–1392.
15. **De Muynck W, Debrouwer D, De Belie N, Verstraete W.** 2008. Bacterial carbonate precipitation improves the durability of cementitious materials. Cement Concrete Res. **38**:1005–1014.
16. **De Muynck W, De Belie N, Verstraete W.** 2010. Microbial carbonate precipitation in construction materials: a review. Ecol. Eng. **36**:118–136.
17. **De Muynck W, Verbeken K, De Belie N, Verstraete W.** 2010. Influence of urea and calcium dosage on the effectiveness of bacterially induced carbonate precipitation on limestone. Ecol. Eng. **36**:99–111.
18. **De Yoreo JJ, Dove PM.** 2004. Shaping crystals with biomolecules. Science **306**:1301–1302.
19. **Dick J, et al.** 2006. Bio-deposition of a calcium carbonate layer on degraded limestone by *Bacillus* species. Biodegradation **17**:357–367.
20. **Doehne E, Price CA.** 2011. Stone conservation: an overview of current research, 2nd ed. Getty Conservation Institute, Los Angeles, CA.
21. **Dupraz S, Parmentier M, Méndez B, Guyot F.** 2009. Experimental and numerical modeling of bacterially induced pH increase and calcite precipitation in saline aquifers. Chem. Geol. **265**:44–53.
22. **Ehrlich HL.** 2002. Geomicrobiology, 4th ed. Marcel Dekker, New York, NY.
23. **Ercole C, Cacchio P, Botta AL, Centi V, Lepidi A.** 2007. Bacterially induced mineralization of calcium carbonate: the role of exopolysaccharides and capsular polysaccharides. Microsc. Microanal. **13**:42–50.
24. **Ferris FG, Stehmeier LG.** September 1992. Bacteriogenic mineral plugging. US patent 5,143,155.
25. **Ferris FG, Fyfe WS, Witten T, Schultze-Lam S, Beveridge TJ.** 1989. Effect of mineral substrate hardness on population density of epilithic microorganisms on two Ontario rivers. Can. J. Microbiol. **35**:744–747.
26. **Fletcher M, Loeb GI.** 1979. Influence of substrate characteristics on the attachments of a marine pseudomonad to solid surfaces. Appl. Environ. Microbiol. **37**:67–72.
27. **Fredd CN, Fogler HS.** 1998. The influence of chelating agents on the kinetics of calcite dissolution. J. Colloid Interface Sci. **204**:187–197.
28. **Gebauer D, et al.** 2010. Proto-calcite and proto-vaterite in amorphous calcium carbonates. Angew. Chem. Int. ed. **49**:8889–8891.
29. **Gollapudi UK, Knutson CL, Bang SS, Islam MR.** 1995. A new method for controlling leaching through permeable channels. Chemosphere **30**: 695–705.
30. **González-Muñoz MT, Rodriguez-Navarro C, Jimenez-Lopez C, Rodriguez-Gallego M.** January 2008. Method and product for protecting and reinforcing construction and ornamental materials. Spanish patent WO 2008/009771 A1.
31. **González-Muñoz MT, et al.** 2011. Bacterial biomineralization: new insights from *Myxococcus*-induced mineral precipitation. Geol. Soc. London Sp. Pub. **336**:31–50.
32. **Gower LB.** 2008. Biomimetic model systems for investigating the amorphous precursor pathway and its role in biomineralization. Chem. Rev. **108**:4551–4627.
33. **Hammes F, Boon N, De Villiers J, Verstraete W, Siciliano SD.** 2003. Strain-specific ureolytic microbial calcium carbonate precipitation. Appl. Environ. Microbiol. **69**:4901–4909.
34. **Harden VP, Harris JO.** 1953. The isoelectric point of bacterial cells. J. Bacteriol. **65**:198–202.
35. **Heijnen WMM.** 1985. The morphology of gel grown calcite. Neues Jahrb. Mineral. **8**:357–371.
36. **Hendricks CW.** 1974. Sorption of heterotrophic and enteric bacteria to glass surfaces in the continuous culture of river water. Appl. Geomicrobiol. **28**:572–578.
37. **Hutchens E.** 2009. Microbial selectivity on mineral surfaces: possible implications for weathering processes. Fungal Biol. Rev. **23**:115–121.
38. **Jimenez-Lopez C, et al.** 2007. Consolidation of degraded ornamental porous limestone by calcium carbonate precipitation induced by the microbiota inhabiting the stone. Chemosphere **68**:1929–1936.
39. **Jimenez-Lopez C, et al.** 2008. Consolidation of quarry calcarenite by calcium carbonate precipitation induced by bacteria activated among the microbiota inhabiting the stone. Int. Biodeterior. Biodegrad. **62**:352–363.
40. **Jroundi F, Fernandez-Vivas A, Rodriguez-Navarro C, Bedmar EJ, Gonzalez-Muñoz MT.** 2010. Bioconservation of deteriorated monumental calcarenite stone and identification of bacteria with carbonatogenic activity. Microb. Ecol. **60**:39–54.
41. **Kawaguchi T, Decho AW.** 2002. A laboratory investigation of cyanobacterial extracellular polymeric secretions (EPS) in influencing $CaCO_3$ polymorphism. J. Cryst. Growth **240**:230–235.
42. **Kim IW, Robertson RE, Zand R.** 2003. Selected polymorphs of $CaCO_3$ through epitaxy with inorganic substrates aligned with an electric field. Adv. Mater. **15**:709–712.
43. **Kitamura M.** 2002. Controlling factor of polymorphism in crystallization process. J. Cryst. Growth **237–239**:2205–2214.
44. **Konhauser KO, et al.** 1994. Mineral precipitation by epilithic biofilms in the Speed River, Ontario, Canada. Appl. Environ. Microbiol. **60**:549–553.
45. **Krumbein WE.** 1974. On the precipitation of aragonite on the surface of marine bacteria. Naturwissenchaften **61**:167.
46. **Krumbein WE.** 1975. Biogenic monohydrocalcite spherules in lake sediments of Lake Kivu (Africa) and the Solar Lake (Sinai). Sedimentology **22**:631–634.
47. **Le Métayer-Levrel G, Castanier S, Orial G, Loubière JF, Perthuisot JP.** 1999. Applications of bacterial carbonatogenesis to the protection and

regeneration of limestones in buildings and historic patrimony. Sediment. Geol. **126**:25–34.
48. **Li H, Xin HL, Muller DA, Estroff LA.** 2009. Visualizing the 3D internal structure of calcite single crystals grown in agarose hydrogels. Science **326**:1244–1247.
49. **Lian B, Hu Q, Chen J, Ji J, Teng HH.** 2006. Carbonate biomineralization by soil bacterium *Bacillus megaterium*. Geochim. Cosmochim. Acta **70**: 5522–5535.
50. **Lioliou MG, Paraskeva CA, Koutsoukos PG, Payatakes AC.** 2007. Heterogeneous nucleation and growth of calcium carbonate on calcite and quartz. J. Colloid Interface Sci. **308**:421–428.
51. **Lippmann F.** 1973. Sedimentary carbonate minerals. Springer-Verlag, Berlin, Germany.
52. **López-Cortés A.** 1999. Paleobiological significance of hydrophobicity and adhesion of phototrophic bacteria from microbial mats. Precambrian Res. **96**:25–39.
53. **Lowenstam HA, Weiner S.** 1989. On biomineralization. Oxford University Press, New York, NY.
54. **Lüttge A, Conrad PG.** 2004. Direct observation of microbial inhibition of calcite dissolution. Appl. Environ. Microbiol. **70**:1627–1632.
55. **Manini E, Luna GM.** 2003. Influence of the mineralogical composition on microbial activities in marine sediments: an experimental approach. Chem. Ecol. **19**:399–410.
56. **Mann S.** 2001. Biomineralization: principles and concepts in bioinorganic materials chemistry. Oxford University Press, Oxford, United Kingdom.
57. **Meldrum F, Cölfen H.** 2008. Controlling mineral morphologies and structures in biological and synthetic systems. Chem. Rev. **108**:4332–4432.
58. **Mitchell AC, Ferris FG.** 2006. The influence of *Bacillus pasteurii* on the nucleation and growth of calcium carbonate. Geomicrobiol. J. **23**:213–226.
59. **Mitchell AC, Dideriksen K, Spangler LH, Cunningham AB, Gerlach R.** 2010. Microbially enhanced carbon capture and storage by mineral-trapping and solubility-trapping. Environ. Sci. Technol. **44**:5270–5276.
60. **Obst M, et al.** 2009. Precipitation of amorphous $CaCO_3$ (aragonite-like) by cyanobacteria: a STXM study of the influence of EPS on the nucleation process. Geochim. Cosmochim. Acta **73**:4180–4198.
61. **Ogino T, Suzuki T, Kawada K.** 1987. The formation and transformation mechanism of calcium carbonate in water. Geochim. Cosmochim. Acta **51**:2757–2767.
62. **Paquette J, Reeder RJ.** 1995. Relationship between surface structure, growth mechanism, and trace element incorporation in calcite. Geochim. Cosmochim. Acta **59**:735–749.
63. **Parkhurst DL, Appelo CAJ.** 1999. User guide to PHREEQC (version 2)—a computer program for speciation, batch reaction, one dimensional transport, and inverse geochemical calculations. U.S. Geological Survey Water-Resources Investigation Report 99-4259. U.S. Geological Survey, Reston, VA.
64. **Pouget EM, et al.** 2009. The initial stages of template-controlled $CaCO_3$ formation revealed by cryo-TEM. Science **323**:1455–1458.
65. **Přikryl R, Svobodová J, Zák K, Hradil D.** 2004. Anthropogenic origin of salt crusts on sandstone sculptures of Prague's Charles Bridge (Czech Republic): evidence of mineralogy and stable isotope geochemistry. Eur. J. Mineral. **16**:609–618.
66. **Ramachandran SK, Ramakrishnan V, Bang SS.** 2001. Remediation of concrete using microorganisms. ACI Mater. J. **98**:3–9.
67. **Rieger J, et al.** 2007. Precursor structures in the crystallization/precipitation processes of $CaCO_3$ and control of particle formation by polyelectrolytes. Farad. Discuss. **136**:265–277.
68. **Rodriguez-Navarro A.** 2006. XRD2DScan: new software for polycrystalline materials characterization using two-dimensional X-ray diffraction. J. Appl. Crystallogr. **39**:905–909.
69. **Rodriguez-Navarro C, Rodriguez-Gallego M, Ben Chekroun K, Gonzalez-Muñoz MT.** 2003. Conservation of ornamental stone by *Myxococcus xanthus*-induced carbonate biomineralization. Appl. Environ. Microbiol. **69**:2182–2193.
70. **Rodriguez-Navarro C, Jimenez-Lopez C, Rodriguez-Navarro A, Gonzalez-Muñoz MT, Rodríguez-Gallego M.** 2007. Bacterially mediated mineralization of vaterite. Geochim. Cosmochim. Acta **71**:1197–1213.
71. **Ruiz-Agudo E, Putnis CV, Jiménez-López C, Rodriguez-Navarro C.** 2009. An atomic force microscopy study of calcite dissolution in saline solutions: the role of magnesium ions. Geochim. Cosmochim. Acta **73**: 3201–3217.
72. **Ruiz-Agudo E, Putnis CV, Wang L, Putnis A.** 2011. Specific effects of background electrolytes on the kinetics of step propagation during calcite growth. Geochim. Cosmochim. Acta **75**:3803–3814.
73. **Sánchez-Navas A, Martín-Algarra A, Rivadeneyra MA, Melchor S, Martín-Ramos JD.** 2009. Crystal-growth behaviour in Ca-Mg carbonate bacterial spherulites. Cryst. Growth Des. **9**:2690–2699.
74. **Scherer GW, Wheeler GS.** 2009. Silicate consolidants for stone. Key Eng. Mater. **391**:1–25.
75. **Scholl MA, Mills AL, Herman JS, Hornberger GM.** 1990. The influence of mineralogy and solution chemistry on the attachment of bacteria to representative aquifer minerals. J. Contamin. Hydrol. **6**:321–336.
76. **Shirakawa MA, Cincotto MA, Atencio D, Gaylarde CC, John VM.** 2011. Effect of culture medium on biocalcification by *Pseudomonas putida*, *Lysinibacillus sphaericus* and *Bacillus subtilis*. Braz. J. Microbiol. **42**:499–507.
77. **Somasundaran P, Agar GE.** 1967. The zero point of charge of calcite. J. Colloid Interface Sci. **24**:142–147.
78. **Sondi I, Sondi BS.** 2005. Influence of the primary structure of enzymes on the formation of $CaCO_3$ polymorphs: a comparison of plant (*Canavalia ensiformis*) and bacterial (*Bacillus pasteurii*) ureases. Langmuir **21**:8876–8882.
79. **Spanos N, Koutsoukos PG.** 1998. The transformation of vaterite to calcite: effect of the conditions of the solution in contact with the mineral phase. J. Cryst. Growth **191**:783–790.
80. **Stocks-Fischer S, Galinat JK, Bang SS.** 1999. Microbiological precipitation of $CaCO_3$. Soil Biol. Biochem. **31**:1563–1571.
81. **Stumm W, Morgan JJ.** 1981. Aquatic chemistry: an introduction emphasizing chemical equilibria in natural waters, 2nd ed. Wiley, New York, NY.
82. **Tai C, Chen FB.** 1998. Polymorphism of $CaCO_3$ precipitated in a constant-composition environment. AIChE J. **44**:1790–1798.
83. **Thompson JB, Ferris FG.** 1990. Cyanobacterial precipitation of gypsum, calcite, and magnesite from natural alkaline lake water. Geology **18**:995–998.
84. **Tiano P, Biagiotti L, Mastromei G.** 1999. Bacterially bio-mediated calcite precipitation for monumental stones conservation: methods of evaluation. J. Microbiol. Methods **36**:139–145.
85. **Tourney J, Ngwenya BT.** 2009. Bacterial extracellular polymeric substances (EPS) mediate $CaCO_3$ morphology and polymorph. Chem. Geol. **262**:138–146.
86. **Urzi C, Garcia-Valles M, Vendrell M, Pernice A.** 1999. Biomineralization processes on rock and monument surfaces observed in field and laboratory conditions. Geomicrobiol. J. **16**:39–54.
87. **Warren LA, Maurice PA, Parmar N, Ferris FG.** 2001. Microbially mediated calcium carbonate precipitation: implications for interpreting calcite precipitation and for solid-phase capture of inorganic contaminants. Geomicrobiol. J. **18**:93–115.
88. **Webster A, May E.** 2006. Bioremediation of weathered-building stone surfaces. Trends Biotechnol. **24**:255–260.
89. **Whiffin VS, van Passen LA, Harkes MP.** 2007. Microbial carbonate precipitation as a soil improvement technique. Geomicrobiol. J. **24**:417–423.
90. **Wingender J, Neu TR, Flemming HC (ed).** 1999. Microbial extracellular polymeric substances: characterization, structure and function. Springer-Verlag, Berlin, Germany.
91. **Wright DT, Oren A.** 2005. Nonphotosynthetic bacteria and the formation of carbonates and evaporites through time. Geomicrobiol. J. **22**:27–53.
92. **Yee N, Fein JB, Daughney CJ.** 2000. Experimental study of pH, ionic strength, and reversibility behavior of bacteria-mineral adsorption. Geochim. Cosmochim. Acta **64**:609–617.
93. **Yoshida N, Higashimura E, Saeki Y.** 2010. Catalytic biomineralization of fluorescent calcite by the thermophilic bacterium *Geobacillus thermoglucosidasius*. Appl. Environ. Microbiol. **76**:7322–7327.
94. **Zamarreño DV, Inkpen R, May E.** 2009. Carbonate crystals precipitated by freshwater bacteria and their use as a limestone consolidant. Appl. Environ. Microbiol. **75**:5981–5990.